Ground-state magneto-optical resonances in Cesium vapour confined in an extremely thin cell

C. Andreeva[1], A. Atvars[2], M. Auzinsh[2], K.Bluss[2],* S. Cartaleva[1], L. Petrov[1], and D. Slavov[1]
[1] *Institute of Electronics - Bulgarian Academy of Sciences, boul. Tzarigradsko shosse 72, 1784 Sofia, Bulgaria*
[2] *Department of Physics and Institute of Atomic Physics and Spectroscopy, University of Latvia, 19 Rainis Blvd., LV-1586 Riga, Latvia*

(Dated: April 23, 2007)

Experimental and theoretical studies are presented related to the ground-state magneto-optical resonance prepared in Cesium vapour confined in an Extremely Thin Cell (ETC, with thickness equal to the wavelength of the irradiating light). It is shown that the utilization of the ETC allows one to examine the formation of a magneto-optical resonance on the individual hyperfine transitions, thus distinguishing processes resulting in dark (reduced absorption) or bright (enhanced absorption) resonance formation. We report on an experimental evidence of the bright magneto-optical resonance sign reversal in Cs atoms confined in the ETC. A theoretical model is proposed based on the optical Bloch equations that involves the elastic interaction processes of atoms in the ETC with its walls resulting in depolarization of the Cs excited state which is polarized by the exciting radiation. This depolarization leads to the sign reversal of the bright resonance. Using the proposed model, the magneto-optical resonance amplitude and width as a function of laser power are calculated and compared with the experimental ones. The numerical results are in good agreement with the experiment.

PACS numbers: 32.80. Qk , 42.50. Gy

I. INTRODUCTION

Recently, the high resolution spectroscopy of alkali atoms confined in a thin cell has proven very promising for the studies not only of atom-light, but also of atom-surface interactions [1]. The realization of such atomic layers has become possible through the development of the so called Extremely Thin Cells (ETC). The ETC consists of a thin layer with a thickness of less than 1 μm and typical diameters of a few centimeters of gas [2], which causes a strong anisotropy in the atom-light interaction.

This anisotropy leads to two main effects in the observed absorption and fluorescence spectra. First, most of the atoms with a velocity component normal to the cell walls collide with the walls before completing the absorption - fluorescence cycle with the incoming light. Hence, these atoms give a smaller contribution to the atomic fluorescence compared to atoms flying parallel to the cell walls. Since generally the light propagation direction is perpendicular to the cell windows, the Doppler broadening of the hyperfine (hf) transitions is significantly reduced. Thus, the hf transitions, which are strongly overlapped in ordinary (cm-size) cells, in the ETC are well resolved with single-beam spectroscopy. Unlike in saturation spectroscopy, the sub-Doppler absorption in an ETC is linear up to relatively large laser power densities, which allows, for example, the determination of transition probabilities of the different hf transitions [3]. The absence of cross-over resonances can also be advantageous when investigating more complex spectra. Second, the investigation of atoms confined in cells whose thickness L is comparable to the wavelength of the light λ leads to the observation of interesting coherent effects. It has been shown that the width of the hf transitions in absorption changes periodically with cell width, with minima at $L = (2n + 1)\lambda/2$ [4], because of the realization of the Dicke regime [5] in the optical domain. Moreover, for the ETC a significant difference in the absorption and fluorescence spectra can be observed because the faster atoms with sufficient interaction time for the absorption of a photon, but not enough for its subsequent release, will contribute to the absorption signal but not to the fluorescence signal [2, 6].

Coherent Population Trapping (CPT) resonances prepared in the Hanle configuration have been widely investigated for Cs and Rb atoms confined in ordinary cells. The alkali atoms, situated in the magnetic field B orthogonal to the atomic orientation/alignment and scanned around $B = 0$, are irradiated by monochromatic laser field in such a configuration that different polarization components of the light couple the atomic Zeeman sublevels of one of the ground-state hf levels through a common excited one and introduce coherence between ground magnetic sublevels at $B = 0$. As has been shown in [7, 8, 9, 10, 11, 12], for degenerate two-level systems in the absence of depolarizing collisions of the excited state, Electromagnetically-Induced Transparency (EIT, dark magneto-optical) resonance or Electromagnetically-Induced Absorption (EIA, bright magneto-optical) resonance can be observed, depending on the ratio of the degeneracies of the two states involved in the optical tran-

*Electronic address: stefka-c@ie.bas.bg

sition. The EIT resonance is realized when the condition $F_g \rightarrow F_e = F_g - 1$, F_g is met, while the EIA resonance is observed for $F_g \rightarrow F_e = F_g + 1$ type of transitions. Here, F_g and F_e are the hf quantum numbers of the ground- and excited-state hf levels, respectively.

The significant disadvantage of magneto-optical resonance studies in ordinary cells is that because of the Doppler broadening in thermal cells, a strong overlapping takes place between hf transitions responsible for dark and bright resonances. Therefore, it is important to make use of the fact that in an ETC the hyperfine transitions are well resolved, and the coherent effects can be investigated under better-defined conditions than in the case of ordinary cells. Moreover, the possibility to separate the contribution of slow and fast atoms to the magneto-optical signal, provided by using the ETC, will result in a better understanding of the transient processes in the formation of the coherent resonances. Besides, magneto-optical resonance investigations in ETCs could give information on the influence of the cell walls on the atomic polarization because, also in the magneto-optical signal, the main contribution is expected from the atoms flying a "long way" along the cell window.

In this work we present experimental and theoretical results concerning the ground-state magneto-optical resonances on the D_2 line of Cs, obtained at the individual hf transitions starting from $F_g = 3$ and $F_g = 4$. It is shown that in the ETC (with thickness equal to the light wavelength), dark (reduced absorption) magneto-optical resonances are observed at $F_g \rightarrow F_e = F_g - 1$, F_g transitions, which is similar to the results obtained in the ordinary cells. A very interesting result is obtained at $F_g \rightarrow F_e = F_g + 1$ transitions. At these transitions, in the dilute Cs vapour confined in the ETC, bright resonance sign reversal is evidenced, which is attributed to the depolarization of the Cs atoms' excited levels. A theoretical model has been developed based on the optical Bloch equations and involving the elastic interaction processes of atoms in an ETC with walls that affect the polarization of the atomic excited levels. The numerical results are in good qualitative agreement with the experimental ones.

II. CESIUM ENERGY LEVELS AND EXPERIMENTAL SETUP

The relevant Cs energy levels and hf transitions involved are illustrated in Fig.1. The two groups of hf transitions (starting from $F_g = 3$ and $F_g = 4$) are denoted. The hf transitions responsible for the formation of magneto-optical resonances of different sign are distinguished. It should be noted that the Doppler broadening ($\sim$ 400 MHz) in the ordinary cell, of the optical hf transitions is larger than the separation between the excited state hf levels. As a result, in the ordinary cell the profiles of the three hf transitions starting from a single ground hf level strongly overlap and form a single

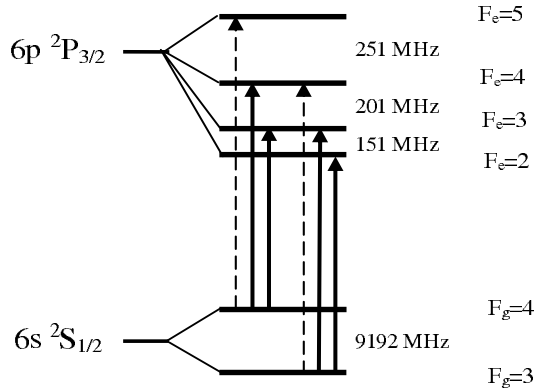

FIG. 1: Energy-level diagram for the D_2 line of ^{133}Cs. $F_g \rightarrow F_e \leq F_g$ transitions (solid line) are distinguished from $F_g \rightarrow F_e > F_g$ transitions (dashed line).

absorption (fluorescence) line. Hence, the three different types of hf transitions, which are responsible for the formation of both dark and bright resonances, are involved in a single fluorescence line. When exciting atoms in the ordinary cell by mono-mode laser light and performing the experiment [12] in dilute Cs vapor (thus avoiding velocity changing collisions between Cs atoms), the three hf transitions forming the fluorescence line will be excited independently, each one at different velocity class of atoms. Under these conditions the open transitions are depleted because of the hf optical pumping to the ground hf level that does not interact with the laser light. Thus they do not play a significant role in the formation of the magneto-optical resonance. At the same time, the closed transition that does not suffer hf optical pumping mainly determines the sign of the magneto-optical resonance. Thus, in the ordinary cells dark resonances are observed at the fluorescence line starting from the $F_g = 3$ and bright resonances at the fluorescence line starting from the $F_g = 4$ levels. The dark resonance observed on the fluorescence line starting from $F_g = 3$ has been attributed to the $F_g = 3 \rightarrow F_e = 2$ closed transition contribution, while the bright resonance is related to the $F_g = 4 \rightarrow F_e = 5$ closed transition.

The experimental setup used is schematically presented in Fig.2a. A cw extended cavity diode laser (ECDL) was used as radiation source. It was operated in single-frequency mode with $\lambda = 852$ nm and linewidth of about 3 MHz. Thus, because of the narrow bandwidth of the laser, it was possible to excite separately the different hyperfine transitions of the D_2 line of ^{133}Cs atoms [$6S_{1/2}(F_g = 3) \rightarrow 6P_{3/2}(F_e = 2, 3, 4)$ or $6S_{1/2}(F_g = 4) \rightarrow 6P_{3/2}(F_e = 3, 4, 5)$]. The main part of the laser beam was directed at normal incidence onto the ETC (zoomed in Fig.2b) with a source containing Cs. The ETC operates with a specially constructed oven which maintains a constant temperature gradient between the Cs atom source (temperature T_1) and the cell windows (temperature T_2), $T_2 > T_1$. The Cs vapour density is controlled by changing the source temperature. The ETC is placed

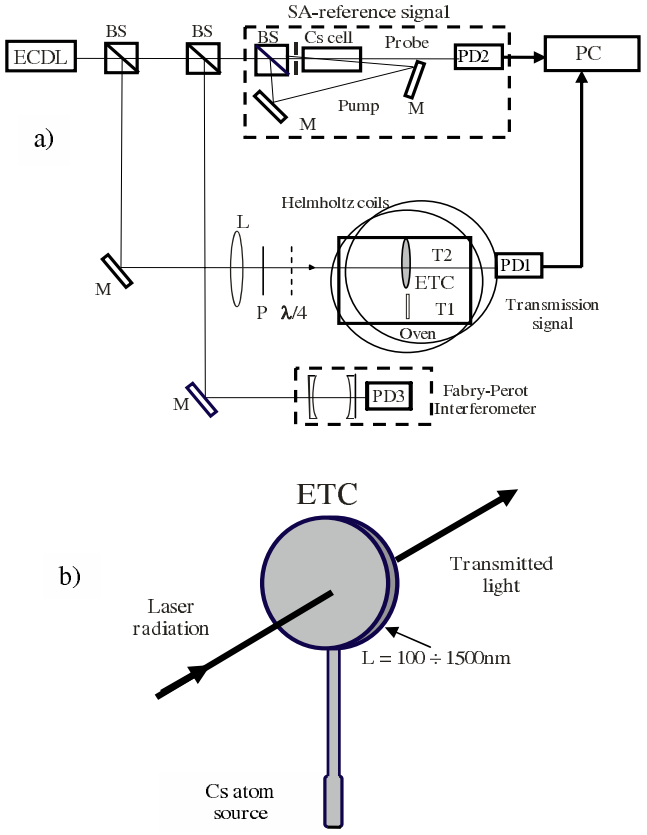

FIG. 2: Experimental set up (a) and sketch of ETC (b).

between a pair of coils in Helmholtz configuration, which allows application of a scanned around $B = 0$ magnetic field in a direction orthogonal to the laser beam propagation direction. No shielding against laboratory magnetic field is provided. The light transmitted through the ETC is measured by photodiode PD1.

Most of the experiments were performed by irradiating Cs atoms by means of linearly polarized light. In this case the scanned magnetic field is oriented in a direction orthogonal to the laser beam and to the light polarization. When light with circular polarization is used, a quarterwave plate is inserted before the ETC, after the polarizer P.

First, an experiment was performed aimed at general observation of the magneto-optical resonance formation along the entire absorption line profile. In this case, the laser frequency was scanned along the absorption profile with a rate of about two orders of magnitude less than that of the magnetic field modulation around $B = 0$. During the second part of the experiment related to the magneto-optical resonance study, the light frequency was fixed at the center of the examined hf transition and Cs atom absorption was measured as a function of the magnetic field, which was scanned around $B = 0$.

The remaining part of the laser beam was separated into two parts and was used for laser frequency control: one part was sent to a scanning Fabry-Perot interferometer in order to monitor the single-mode operation of the ECDL and the second one to an additional branch of the setup including an ordinary, 3 cm long Cs cell, for simultaneous registration of the Saturated Absorption (SA) spectrum, which was used for precise scaling and reference of the laser frequency.

III. ABSORPTION SPECTRA AT THE ETC THICKNESS L=λ/2 AND L=λ

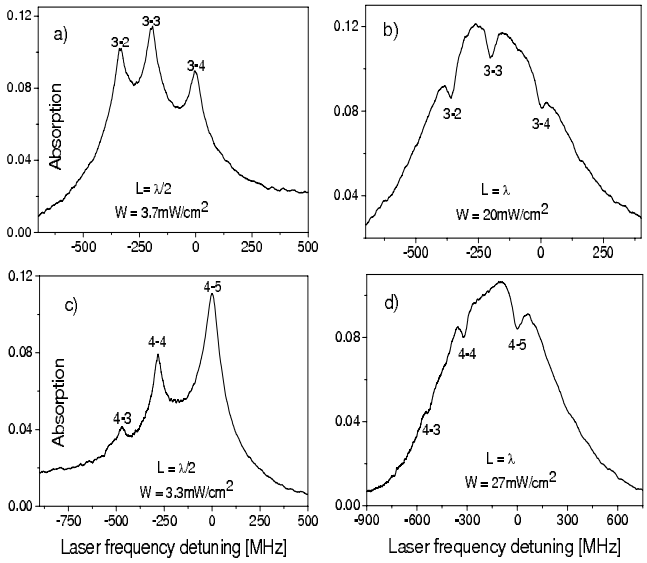

FIG. 3: Absorption spectra at F_g=3 (a,b) and $F_g = 4$ (c,d) sets of hf transitions, for ETC thickness L=λ /2 (a,c) and $L = \lambda$ (b,d).

In order to help the further discussion related to magneto-optical resonances observed in the ETC, in this Section we present the absorption spectra of both absorption lines at two thicknesses of the ETC (Fig.3), observed without application of the magnetic field. For $L = \lambda/2$, the absorption spectra of the lines starting from $F_g = 3$ and $F_g = 4$ are illustrated in Fig.3a,c. It can be seen that the spectral profiles of all hf transitions are well resolved due to the significant enhancement of atomic absorption at the hf transition center and its reduction toward the wings. As was mentioned in the introduction, the origin of the narrowing of the hf transition profiles is attributed to the Dicke effect. The processes responsible for the coherent Dicke narrowing of the hf transition profile at $L = \lambda/2$ can be briefly summarized as follows [4, 6, 13]. If an atom at the moment of leaving the cell wall is excited by resonant light, the excitation will start to precess in phase with the exciting electromagnetic field at the wall position. However, with the atomic motion the excitation will drift gradually out of phase with the local exciting field. The phase mismatch appearing on the line center under a weak exciting field is independent of the atomic velocity and, for a cell thickness up to $\lambda/2$, all regions of the cell

interfere constructively, leading to a strong absorption enhancement at the hf transition center. However, if the exciting light is detuned from the hf transition center, the angular precession of the atomic excitation becomes velocity-dependent resulting in a smooth reduction of the absorption in the wings of the hf profile.

Unlike the atomic spectra observed at L = $\lambda/2$, when the cell thickness rises up to L = λ, a completely different behaviour of the hf transition absorption occurs (Fig.3b, d). Under this condition the Dicke narrowing vanishes and at low light power density the Dopler profiles of hf transitions forming the fluorescence line are completely overlapped. However, starting from a power density W of several mW/cm^2, narrow dips of reduced absorption occur, centered at each hf transition. The observed dips are attributed to velocity-selective saturation of the hf transition and to velocity-selective population loss due to optical pumping to the ground-state level that does not interact with the exciting light field. To complete saturation and/or optical pumping, the atom needs a longer interaction time with the exciting light than for a single act of absorption [14]. Due to this, primarily the very slow atoms or those flying parallel to the ETC windows can contribute to the reduced absorption dips at L = λ. Note that it is expected that the latter group of atoms will be responsible for the magneto-optical resonance formation, because this process is also slower than ordinary linear absorption.

IV. MAGNETO-OPTICAL RESONANCES OBSERVATION IN AN ETC WITH THICKNESS L = λ: THE BRIGHT RESONANCE SIGN REVERSAL

As shown in the previous section, an important advantage of using the ETC is that it is possible to study the behaviour of the individual hf transitions. In order to test this property, the following experiment is performed related to the magneto-optical resonances. The laser frequency is slowly scanned over the hf transition profile. During this slow scan, the magnetic field is scanned around $B = 0$ with a frequency about two orders of magnitude higher than the frequency of laser scan. Such an experiment allows the observation of a sequence of magneto-optical resonances superimposed on the absorption profile of the transition registered during the laser frequency detuning. The minimum absorption of the dark resonances and the maximum absorption of the bright resonances are observed at $B = 0$. First, the magneto-optical resonances at the three hf transitions starting from the $F_g = 3$ level are examined (Fig.4). In order to determine precisely the $B = 0$ points, magneto-optical resonances are simultaneously registered in the ordinary cell used for SA resonance observation (Fig.4, solid lines). The ordinary cell is situated outside the Helmholtz coils, so the magnetic field from the Helmholtz coils there is not homogeneous and its value is lower than

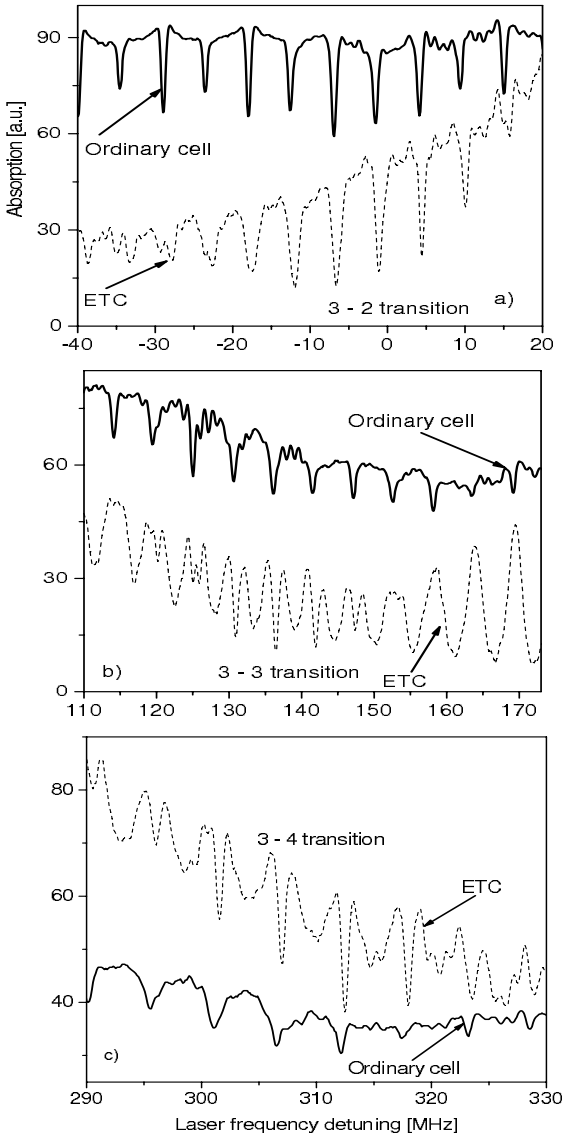

FIG. 4: Magneto-optical resonances superimposed on the ETC absorption (dashed line) obtained by slow laser frequency detuning in small intervals around the centers of $F_g = 3 \rightarrow F_e = 2$ (a), $F_g = 3 \rightarrow F_e = 3$ (b) and $F_g = 3 \rightarrow F_e = 4$ (c) transitions. A magnetic field is applied and scanned around $B = 0$ with a frequency two orders of magnitude higher than that of the laser frequency scan. For comparison of the $B = 0$ positions, a simultaneous recording of the resonances in ordinary cell is shown (solid line). Cs source temperature is 120^{o}C, ETC thickness L = λ and laser power - 66mW/cm^2. Cs atoms are irradiated by linearly polarized laser light.

that applied to the ETC. Hence, it is not possible to compare the widths of magneto-optical resonances observed in both cells but the determination of the $B = 0$ points is correct.

Fig.4a illustrates the fact that magneto-optical dark resonances are observed in a region of several tens of MHz around the $F_g = 3 \rightarrow F_e = 2$ transition center.

This interval is significantly narrower than the Doppler width of the corresponding hf transition. The sign of the magneto-optical resonance observed in the ETC corresponds to that observed in an ordinary cell. A dark resonance is observed at the $F_g = 3$ $F_e = 3$ transition (Fig.4b), and it also exists in a narrow region around the hf transition center. For this transition, the resonance sign is also in agreement with the observations in ordinary cells. From Fig.4b it can be seen that the dark resonance observed for slow atoms is superimposed on some other feature. The full profile of this feature can be clearly distinguished for the atoms faster than those contributing to the absorption around the hf transition center. This type of Cs absorption dependence on the magnetic field, which is broader than the dark resonance, has a maximum at $B = 0$ and is not related to coherent superposition of atomic levels, will be discussed in more detail later in this Section.

As mentioned in the introduction, bright resonances are observed at $F_g \rightarrow F_e = F_g + 1$ transitions of dilute alkali atoms contained in the ordinary cells, where the collisions between atoms can be neglected. Due to this, in the ETC, a narrow bright resonance was expected for the $F_g = 3 \rightarrow F_e = 4$ transition. However, at the intrinsically "bright" $F_g = 3 \rightarrow F_e = 4$ transition, a dark resonance is observed in the ETC. It should be pointed out that the $F_g = 3 \rightarrow F_e = 4$ transition is an open one with a transition probability significantly less than that of the closed $F_g = 3 \rightarrow F_e = 2$ transition. As a result, in the ordinary cell it was not possible to observe magneto-optical resonances determined by this transition.

In order to obtain more information about the behaviour of the $F_g \rightarrow F_e = F_g + 1$ type of transitions in the ETC, the $F_g = 4$ set of transitions was investigated where the $F_g = 4 \rightarrow F_e = 5$ transition is closed and is the strongest one. The obtained results are presented in Fig.5 where only the ETC signal is shown (in the presence and in the absence of the magnetic field). In the first case (Fig.5, solid line), the $B = 0$ points are not noted and we will specify the magneto-optical resonance sign. At low light power (Fig.5a), the above mentioned broader features predominate over the whole region of the presented absorption spectrum, including the central regions of the three hf transitions . At the centers of the hf transitions, only very small-amplitude dark magneto-optical resonances are observed superimposed on the tops of the profiles having maxima at $B = 0$. When increasing the light power (Fig.4b), the dark resonance amplitude increases and, as in the case of the $F_g = 3$ set of transitions, they are observed in a narrow interval around the center of the hf transitions. More specifically, the magneto-optical resonances are observed only within the frequency intervals where the reduced absorption dips occur in the Cs absorption spectrum at L = λ (Fig.5, dashed curve obtained at $B = 0$). In the remaining regions of the light frequency scan, the above mentioned features, which are assumed to be of non-coherent origin are observed. Our experiment has shown that for very

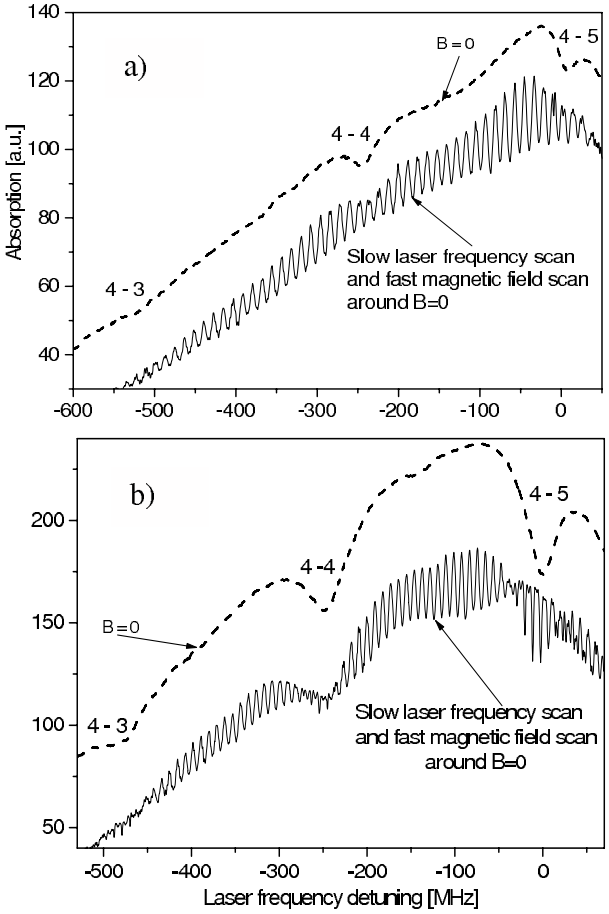

FIG. 5: Magneto-optical resonances superimposed on the ETC absorption spectrum (solid line) and the corresponding part of the ETC absorption spectrum (dashed line) at the $F_g = 4$ absorption line for two different laser powers W=13mW/cm^2 (a) and W=133mW/cm^2 (b). Cs source temperature is 131^{o}C, L =λ, linearly polarized laser light.

low laser power, these features are observed over the entire absorption spectra of both $F_g = 3$, 4 sets of hf transitions. Hence, the discussed features appear only under conditions sufficient for the realization of single-photon absorption. As the formation of the magneto-optical resonance requires alignment/orientation of atoms (including several absorption-fluorescence cycles), which is a much longer process, we believe that the formation of the non-coherent origin feature is related to the large magnetic field scan (-90 G, +90 G) needed to register the magneto-optical resonance. To understand this effect, suppose that the laser light is in resonance with a certain velocity class of atoms. As the width of the irradiating light is small (3 MHz), only at $B = 0$ all transitions starting from different Zeeman sublevels will be in exact resonance with the laser light. Taking into consideration the Zeeman splitting of the ground state (0.35 MHz/G) and the excited state (0.93 MHz/G for $F_e = 2$, 0.00 for $F_e = 3$, 0.37 MHz/G for $F_e = 4$, 0.56 MHz/G for $F_e = 5$) levels, it can be estimated that the magnetic

field increase will result in a significant shift from the laser light frequency of the centers of optical transitions that start from different ground-state Zeeman sublevels. Those shifts will be proportional to the m_F value, and only the $m_{F_g} = 0 \rightarrow m_{F_e} = 0$ transitions will stay in resonance with the laser light during the magnetic field scan.

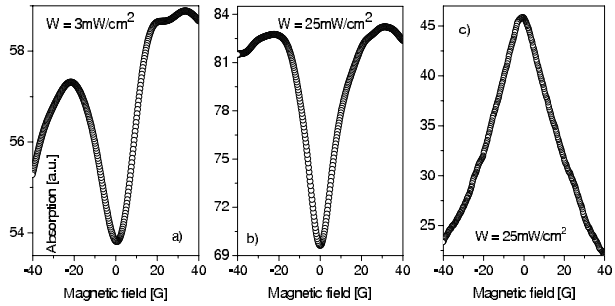

FIG. 6: Illustration of dark magneto-optical resonances observed at $F_g = 3 \rightarrow F_e = 2$ (a) and $F_g = 3 \rightarrow F_e = 4$ (b) transitions for slow atoms, and non-coherent feature (c) observed for fast atoms. Cs source temperature is 112^{o}C and L $= \lambda$.

In general, the shifts of centers of different transitions are significant compared to their natural width and might be considered as a reason why the Cs atom absorption is reduced as the magnetic field is detuned from zero-value, thus forming features in the absorption dependence on magnetic field with maxima at $B = 0$. In this way, we attribute the discussed features to the non-coherent dependence of absorption on the magnetic field, whose origin are the shifts of the Zeeman transition centers from the light frequency with the magnetic field scan. Hence, only slow atoms, which suffer optical pumping and saturation, are also involved in the formation of the magneto-optical resonances. Fast atoms, which exhibit much shorter interaction time with the light, are mainly responsible for the appearance of the non-coherent feature .

Fig.6 illustrates the dependance of the magneto-optical resonance and the non-coherent feature on magnetic field. The dark magneto-optical resonance that is observed for slow atoms at all $F_g \rightarrow F_e = F_g - 1, F_g$ transitions is illustrated in Fig.6a, for the closed $F_g = 3 \rightarrow F_e = 2$ transition. In Fig.6b, the dark magneto-optical resonance that is observed in case of slow atoms at the $F_g = 3 \rightarrow F_e = 4$ transition is shown. The case of fast atoms is illustrated in Fig.6c. Similar results are observed by irradiating Cs atoms with circularly polarized light and applying a magnetic field orthogonal to the laser beam .

Coming back to Fig.5b, it should be particularly stressed that for the closed $F_g = 4 \rightarrow F_e = 5$ transition, also a dark resonance is evidenced in the case of the ETC. This result is very interesting, because precisely for this transition a very well resolved bright resonance is observed in the ordinary cell, which contains dilute Cs atoms [12]. However, it turns out that the bright resonance is very sensitive to the buffering of the ordinary cell. It has been found [12] and very recently confirmed [15, 16] that if the cell containing alkali atoms is buffered by some noble gas, the magneto-optical resonance at the $F_g = 4 \rightarrow F_e = 5$ transition is changed from a bright to a dark one. The theoretical modeling has shown that this transformation of the resonance sign can be attributed to the depolarization of the F_e level by collisions of alkali atoms with the buffer gas atoms. At the same time, these collisions do not lead to depolarization of the F_g level, thus preserving the coherent superposition of the ground-state magnetic sublevels introduced by the light at $B = 0$. Note that the ordinary cell buffering does not reverse the sign of the dark magneto-optical resonances observed on the $F_g \rightarrow F_e = F_g - 1, F_g$ type of transitions.

To easily picture the physical processes that lead to the magneto-optical resonance sign reversal due to collisions between alkali and buffer gas atoms in the ordinary cell, it is better to consider Cs atoms irradiated by circularly polarized light. In this case, the magneto-optical resonance is observed in absorption (fluorescence) as a function of the magnetic field orthogonal to the laser beam and scanned around $B = 0$. Let us consider the $F_g = 4 \rightarrow F_e = 5$ transition on the D_2 line of Cs (Fig.7). In the absence of depolarizing collisions and in the presence of circularly polarized light (σ^+), because the Clebsch Gordon coefficients increase for transitions starting from $m_{F_g} = -4$ to $m_{F_g} = 4$, most atoms will circulate on the $m_{F_g} = 4 \rightarrow m_{F_e} = 5$ transition, which is the transition with the highest probability of absorption for σ^+ polarization. Therefore, at $B = 0$ a maximum in the absorption (fluorescence) will be observed. In the presence of the magnetic field perpendicular to the atomic orientation, part of the population of the $m_{F_g} = 4$ sublevel will be redistributed to the other sublevels and the absorption (fluorescence) will be decreased, which results in the observation of a narrow resonance of enhanced absorption (fluorescence) determined as a bright magneto-optical resonance. However, if a buffer gas is added, a large fraction of the atoms accumulated on the $m_{F_e} = 5$ sublevel will be redistributed among the other Zeeman sublevels of the $F_e = 5$ level because of the depolarizing collisions between Cs and buffer gas atoms. Taking into account the difference in the probabilities of the transitions between the different Zeeman sublevels, it has been shown [12] that this redistribution leads to an accumulation (at $B = 0$) of many atoms on the $m_{F_g} = -4$ sublevel, having the lowest probability for σ^+ excitation. Thus, the bright resonance observed in pure and dilute Cs vapour transforms into a dark one when buffer gas is added to the ordinary cell.

In analyzing the results related to the bright resonance sign reversal due to the depolarization of the excited state, an assumption has been made that in the ETC a similar depolarization of the excited state can occur due to the long-range interaction between alkali atoms and the two window surfaces of the ETC. In support of such an assumption, note that during their interaction with the light, atoms responsible for the magneto-optical

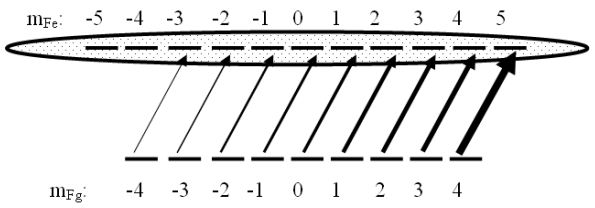

FIG. 7: Illustration of the transformation of bright to dark resonance at the $F_g = 4 \rightarrow F_e = 5$ transition, in case of depolarizing $F_e = 5$ level collisions between Cs and buffer gas atoms.

resonance formation fly a "long way" (on the order of a millimeter) along the ETC windows, which are separated only by a tiny gap very close to 852 nm. As an additional support to this assumption, we report here the results of our measurement of the polarization of the fluorescence collected in a direction orthogonal to the laser beam. While in ordinary cell containing pure Cs we measured a degree of fluorescence polarization $P = 0.24$, in the ETC significant depolarization of the fluorescence was observed yielding $P = 0.02$. A theoretical model has been developed to analyze the experimental observations that will be presented in the following Section.

V. THEORETICAL MODEL

A. Introduction and definitions

We consider the dipole interaction of an atom with a laser field in presence of an external static magnetic field $\mathbf{B}$. We assume that the atomic center of mass moves classically, which means that the only effect of the dipole interaction of the atom with the laser field is an excitation of a classically moving atom at the internal transitions. In this case the internal atomic dynamics is described by the semiclassical atomic density matrix ρ, which parametrically depends on the classical coordinates of the atomic center of mass.

We are interested in the optical Bloch equations (OBE) for the density matrix elements $\rho_{g_i g_j}, \rho_{g_i e_j}, \rho_{e_i g_j}, \rho_{e_i e_j}$, where g_i and g_j label atomic ground-state magnetic sublevels, and e_i and e_j excited-state magnetic sublevels. In writing the OBEs (see, for example, [17]),

$$\imath\hbar\frac{\partial\rho}{\partial t} = \left[\widehat{H},\rho\right] + \imath\hbar\widehat{R}\rho, \tag{1}$$

we consider the relaxation $\widehat{R}$ due to spontaneous emission, transit relaxation and due to interaction of atoms with the cell walls – both in non-elastic and elastic collisions. We also assume, that different velocity groups do not mix in atom – atom as well as atom – wall interactions, since the atomic density is sufficiently low.

The Hamiltonian

$$\widehat{H} = \widehat{H_0} + \widehat{H_B} + \widehat{V} \tag{2}$$

includes the unperturbed atomic Hamiltonian $\widehat{H_0}$, which depends on the internal atomic coordinates: $\widehat{H_0}\left|\Psi_n\right\rangle = E_n\left|\Psi_n\right\rangle$, $\widehat{H_B}$, the interaction of an atom with the external magnetic field $\mathbf{B}$, and the dipole interaction operator $\widehat{V} = -\widehat{\mathbf{d}}\cdot\mathbf{E}(t)$, where $\widehat{\mathbf{d}}$ is the electric dipole operator. The exciting light is described classically by a fluctuating electric field $\varepsilon(t)$ of definite polarization $\mathbf{e}$:

$$\mathbf{E}(t) = \varepsilon(t)\,\mathbf{e} + \varepsilon^*(t)\,\mathbf{e}^* \tag{3}$$

$$\varepsilon(t) = \left|\varepsilon_{\overline{\omega}}\right| e^{-\imath\Phi(t)-\imath(\overline{\omega}-\mathbf{k}_{\overline{\omega}}\mathbf{v})t} \tag{4}$$

with the center frequency of the spectrum $\overline{\omega}$ and the fluctuating phase $\Phi(t)$, which gives the spectrum a finite bandwidth $\Delta\omega$. The lineshape of the exciting light is Lorentzian with FWHM $\triangle\omega$.

B. Optical Bloch equations

Writing OBEs explicitly for the density matrix element ρ_{ij}, we get:

$$\begin{aligned}
\frac{\partial\rho_{ij}}{\partial t} &= -\frac{\imath}{\hbar}\left[\widehat{H},\rho_{ij}\right] + \widehat{R}\rho_{ij} = -\frac{\imath}{\hbar}\left[\widehat{H_0},\rho_{ij}\right] + \frac{\imath}{\hbar}\left[\widehat{\mathbf{d}}\cdot\mathbf{E}(t),\rho_{ij}\right] + \widehat{R}\rho_{ij} = \\
&= -\imath\omega_{ij}\rho_{ij} + \frac{\imath}{\hbar}\mathbf{E}(t)\sum_k\left(\mathbf{d}_{ik}\cdot\rho_{kj} - \rho_{ik}\cdot\mathbf{d}_{kj}\right) + \widehat{R}\rho_{ij} = \\
&= -\imath\omega_{ij}\rho_{ij} + \frac{\imath}{\hbar}\varepsilon(t)\sum_k d_{ik}\rho_{kj} + \frac{\imath}{\hbar}\varepsilon^*(t)\sum_k d^*_{ik}\rho_{kj} - \frac{\imath}{\hbar}\varepsilon(t)\sum_k d_{kj}\rho_{ik} - \frac{\imath}{\hbar}\varepsilon^*(t)\sum_k d^*_{kj}\rho_{ik} + \widehat{R}\rho_{ij}
\end{aligned} \tag{5}$$

where $\omega_{ij} = \dfrac{E_i - E_j}{\hbar}$, and the transition dipole matrix elements $d_{ij} = \langle i\left|\mathbf{d}\right|j\rangle$ and $d_{ij} = \langle i\left|\mathbf{d}\cdot\mathbf{e}\right|j\rangle$ can be calculated using the standard angular momentum algebra [18, 19, 20].

C. Simplification of the OBEs

Next, we apply the following procedure, which simplifies OBE. First, we use the rotating wave approximation [21]. After that we have the equations, which are stochastic differential equations [22] with stochastic variable $\frac{\partial\Phi(t)}{\partial t}$. In experiment we measure time averaged (stationary) values. Therefore, we need to perform the statistical averaging of the above equations. In order to do that, we solve the equations for optical coherences and then take a formal statistical average over the fluctuating phases. Finally we apply the "decorrelation approximation" (which in general is valid only for Wiener-Levy-type phase fluctuations) and assume a "phase diffusion" model for the description of the dynamics of the fluctuating phase. Thus we obtain a phase averaged OBE. For a detailed description of the procedure of statistical averaging, decorrelation approximation, Wiener-Levy-type phase fluctuations, and phase-diffusion model, see [23] and references cited therein.

D. Steady-state excitation

Now we assume, that atoms in the cell reach the stacionary excitation conditions (steady-state). Under such conditions all density matrix elements in the OBE become time independent. In these conditions we can eliminate the optical coherences $\rho_{g_ie_j}$ and $\rho_{e_ig_j}$ [14, 17] from OBE. Thus, for optical coherences we obtain the following explicit expressions:

$$\widetilde{\rho_{g_ie_j}} = \frac{\imath}{\hbar}\frac{|\varepsilon_{\overline{\omega}}|}{\Gamma_R + \imath\Delta_{e_jg_i}}\left(\sum_{e_k} d^*_{g_ie_k}\rho_{e_ke_j} - \sum_{g_k} d^*_{g_ke_j}\rho_{g_ig_k}\right) \tag{6}$$

$$\widetilde{\rho_{e_ig_j}} = \frac{\imath}{\hbar}\frac{|\varepsilon_{\overline{\omega}}|}{\Gamma_R - \imath\Delta_{e_ig_j}}\left(\sum_{g_k} d_{e_ig_k}\rho_{g_kg_j} - \sum_{e_k} d_{e_kg_j}\rho_{e_ie_k}\right), \tag{7}$$

where

$$\Delta_{ij} = \overline{\omega} - \mathbf{k}_{\overline{\omega}}\mathbf{v} - \omega_{ij} \tag{8}$$

and $\mathbf{k}_{\overline{\omega}}\mathbf{v}$ represents the Doppler shift of the transition energy of an atom due to its spatial motion. Here $\mathbf{k}$ is the wave vector of the excitation light and $\mathbf{v}$ is the atom velocity. In the present study it was assumed that in the ETC $\mathbf{k}_{\overline{\omega}}\mathbf{v} = 0$. Γ_R describes effective relaxation,

$$\Gamma_R = \frac{\Gamma}{2} + \frac{\Delta\omega}{2} + \gamma + \Gamma_{col}, \tag{9}$$

where Γ describes spontaneous relaxation from level e, γ describes the relaxation rate, $\Delta\omega$, the relaxation due to finite linewidth of the laser (this relaxation is the consequence of the statistical averaging over the laser field fluctuations), and Γ_{col} describes the relaxation due to elastic atomic collisions with the cell walls.

E. Rate equations for Zeeman coherences

By substituting the expressions for the optical coherences Eqs. (6, 7) in the equations for the Zeeman coherences, we arrive at the rate equations for Zeeman coherences only (see [23]):

$$\begin{aligned}\frac{\partial\rho_{g_ig_j}}{\partial t} \;=\; 0 = {} & -\imath\omega_{gigj}\rho_{g_ig_j} - \gamma\rho_{g_ig_j} + \sum_{e_ie_j}\Gamma^{e_ie_j}_{g_ig_j}\rho_{e_ie_j} + \lambda\delta(g_i,g_j) + \\ & + \frac{|\varepsilon_{\overline{\omega}}|^2}{\hbar^2}\sum_{e_k,e_m}\left(\frac{1}{\Gamma_R + \imath\Delta_{e_mg_i}} + \frac{1}{\Gamma_R - \imath\Delta_{e_kg_j}}\right)d^*_{g_ie_k}d_{e_mg_j}\rho_{e_ke_m} - \\ & - \frac{|\varepsilon_{\overline{\omega}}|^2}{\hbar^2}\sum_{e_k,g_m}\left(\frac{1}{\Gamma_R - \imath\Delta_{e_kg_j}}d^*_{g_ie_k}d_{e_kg_m}\rho_{g_mg_j} + \frac{1}{\Gamma_R + \imath\Delta_{e_kg_i}}d^*_{g_me_k}d_{e_kg_j}\rho_{g_ig_m}\right)\end{aligned} \tag{10}$$

$$\frac{\partial \rho_{e_i e_j}}{\partial t} = 0 = -\imath\omega_{e_i e_j}\rho_{e_i e_j} - \gamma\rho_{e_i e_j} - \Gamma\rho_{e_i e_j} - \Gamma_{col}\rho_{e_i e_j} + \\ +\Gamma_{col}\cdot\delta\left(e_i,e_j\right)\cdot\sum_{e_k}\frac{N_{e_k e_i}}{\sum\limits_{e_m} N_{e_k e_m}}\rho_{e_k e_k} + \\ +\frac{|\varepsilon_{\overline{\omega}}|^2}{\hbar^2}\sum_{g_k,g_m}\left(\frac{1}{\Gamma_R - \imath\Delta_{e_i g_m}} + \frac{1}{\Gamma_R + \imath\Delta_{e_j g_k}}\right) d_{e_i g_k} d^*_{g_m e_j}\rho_{g_k g_m} - \\ -\frac{|\varepsilon_{\overline{\omega}}|^2}{\hbar^2}\sum_{g_k,e_m}\left(\frac{1}{\Gamma_R + \imath\Delta_{e_j g_k}} d_{e_i g_k} d^*_{g_k e_m}\rho_{e_m e_j} + \frac{1}{\Gamma_R - \imath\Delta_{e_i g_k}} d_{e_m g_k} d^*_{g_k e_j}\rho_{e_i e_m}\right) \quad (11)$$

Here $\Gamma^{e_i e_j}_{g_i g_j}$ describes the spontaneous relaxation from $\rho_{e_i e_j}$ to $\rho_{g_i g_j}$, λ describes the rate at which "fresh" atoms move into interaction region in the transit relaxation process, $\delta\left(i,j\right)$ is the Dirac delta symbol, but N_{ij} describes the relative rate of the elastic interaction of atoms with the walls of the ETC:

$$N_{ij} = \frac{\Delta^2_{col}}{\Delta^2_{col} + |\omega_{ij}|^2} \quad (12)$$

F. Model for elastic collisions

When atoms move through the cell, they may experience elastic and inelastic interactions with the walls of the ETC. As was shown in [1], the ETC provides the possibility to explore the long-range atom-surface van der Waals interaction and modification of atomic dielectric resonant coupling under the influence of the coupling between the two neighboring dielectric media, and even the possible modification of interatomic collision processes under the effect of confinement. Besides, if an atom is "flying" very close to the surface, it can even experience the periodic potential coming from the crystalline surface of the ETC. We will speak about these effect as the effect of elastic collisions occurring with the rate Γ_{col}.

We assume the following model for elastic collisions. First, these collisions do not affect ground state (Eq. 10), as in the ground state $L_g = 0$, and we assume that these collisions cannot "turn" the spin – neither electronic spin S, nor nuclear spin I. Thus, collisions affect excited-state Zeeman coherences and populations (Eq. 11), as well as optical coherences Eqs. (6, 7).

The second assumption is that elastic collisions redistribute populations only among excited-state magnetic sublevels, see Eq. (11), which means that both the optical coherences and the excited-state Zeeman coherences are destroyed completely with the rate Γ_{col}.

Finally we want to note that the external **B**-field not only causes magnetic sublevel splitting $\omega_{e_i e_j}$ and $\omega_{g_i g_j}$, but also alters the dipole transition matrix elements by mixing the hf levels with the same magnetic quantum number m, but with different hf level angular momentum quantum number F.

$$|e_i\rangle = \sum_{F_e} c^{(e)}_i |F_e m_i\rangle \quad (13)$$

$$|g_i\rangle = \sum_{F_g} c^{(g)}_i |F_g m_i\rangle \quad (14)$$

The numerical values of the magnetic sublevel splitting energies $\omega_{e_i e_j}$ and $\omega_{g_i g_j}$, as well as the hf state mixing coefficients $c^{(e)}_i$ and $c^{(g)}_i$ are obtained by diagonalization of the magnetic field interaction Hamiltonian $\widehat{H_B}$ Eq. (2).

The third assumption is the phenomenological model for the redistribution of the excited-state population due to collisions, namely Eq. (12). The quantity $\sum_{e_m} N_{e_k e_m}$ in Eq. (11) is the normalization coefficient. As can be seen from Eq. (12), we assume that the distribution of the probability for the atomic interaction with the ETC walls to mix populations in the excited state of the atoms has a Lorentzian shape with FWHM Δ_{col} . Thus Δ_{col} could be called the effective width of the elastic collisions.

VI. COMPARISON BETWEEN THEORETICAL AND EXPERIMENTAL RESULTS

Based on the model developed for the ETC, the magneto-optical resonance profiles have been computed for laser frequency detuning over all hf transitions and for both types of excitations, that is, by linearly and circularly polarized light. In the calculations, the following parameters related to the experimental conditions have been used: Γ = 6 MHz, γ = 5 MHz, $\Delta\omega$ = 3 MHz, Γ_{col} = 200 MHz, Δ_{col} = 50 MHz.

In all the cases considered, the theoretical results are at least in qualitative agreement with the experimental observations. As in the experiment, reduced absorption magneto-optical resonances are predicted by the theory for all $F_g \to F_e = F_g - 1$, F_g transitions.

The inclusion in the theoretical model of the influence of the cell walls on the polarization of the excited atomic level has as a result the sign reversal of the bright

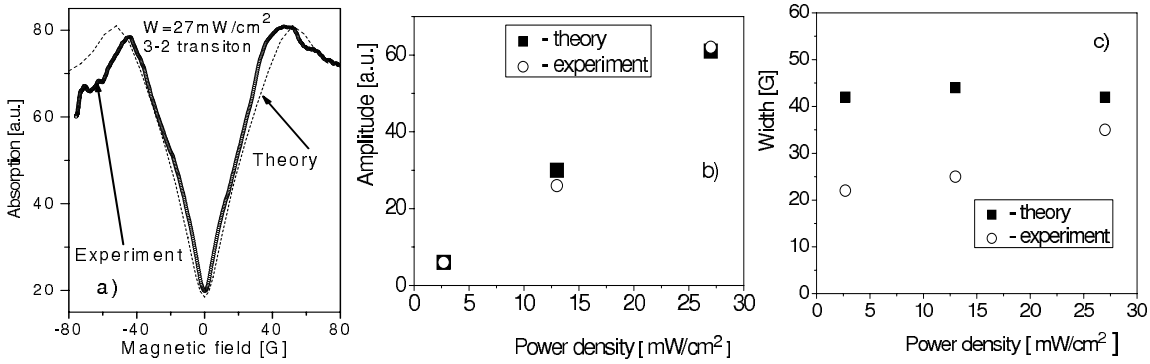

FIG. 8: Comparison between theory and experiment, for $F_g = 3 \rightarrow F_e = 2$ transition and excitation by linearly polarized light: (a) - magneto-optical resonance experimental and theoretical profiles; (b) - magneto-optical resonance amplitude as function of the light power density; (c) - magneto-optical resonance width as a function of power density.

magneto-optical resonance. Mixing of the excited state Zeeman sublevels according to Eq. (11) and (12) is assumed, which results in atomic accumulation in the ground-state Zeeman sublevels with the lowest probability of excitation (at $B = 0$) for the $F_g \rightarrow F_e = F_g+1$ transitions. This atomic accumulation in "the less favored" ground sublevel is the reason for the bright magneto-optical resonance sign reversal. The experimentally observed reduced-absorption magneto-optical resonances at this type of transition supports our theoretical result. We would like to remind the reader, that in the case of the $F_g \rightarrow F_e = F_g + 1$ transitions, without the cell window influence, atomic excitation by light of any polarization would results in atomic accumulation in the ground-state Zeeman sublevel with the highest probability of excitation (at $B = 0$), and hence in the observation of enhanced-absorption, bright magneto-optical resonance.

Let us discuss the behaviour of particular magneto-optical resonances when the laser frequency is tuned to the central frequencies of the different hf transitions. In an interval of a few tens of MHz around the $F_g = 3 \rightarrow F_e = 2$ transition, a dark resonance is experimentally observed and is shown in Fig.8 together with the theoretically simulated profile of the resonance. Here, Cs atoms are irradiated by linearly polarized light and the magnetic field is orthogonal to the polarization vector and to the light propagation direction. A good quantitative agreement between the theoretical and the experimental results can be seen. The resonance amplitude increases with the light power density and here the agreement of the theory with the experiment is very good. Some discrepancy still remains between the theoretical and experimental resonance widths for low laser power, which can be due to the residual Doppler broadening not accounted for in the model. When the laser power is increased, the transition saturation effects start to dominate over the Doppler broadening. The $F_g = 3 \rightarrow F_e = 3$ transition behaves similar to that of the $F_g = 3 \rightarrow F_e = 2$ transition. Here also a dark magneto-optical resonance is observed, and also the theoretical profile parameters are in agreement with those of the experimental profiles.

It should be pointed out that the magneto-optical resonance width in the ETC is an order of magnitude larger than that obtained in the ordinary cell. This broadening can be attributed to the larger value of the transit relaxation rate due to the nanometric scale of the ETC thickness as compared to the cm-dimensions of the ordinary cell. Note that the ETC is not shielded against the laboratory magnetic field because of technical reasons connected with its shape and because the magnetic field must be scanned in quite a large interval. But as the laboratory magnetic field is less than a Gauss, the lack of shielding should not influence significantly the resonance width. Moreover, an experiment with an unshielded ordinary cell situated very close to the ETC shows a magneto-optical resonance with less than 1 G width, which proves that the laboratory magnetic field cannot be the main reason for the resonance broadening.

The $F_g = 3 \rightarrow F_e = 4$ transition represents an interesting case. As mentioned above for the case of the ordinary cell, because of the strong overlapping of the Doppler profiles of the hf transitions and the weakness of the $F_g = 3 \rightarrow F_e = 4$ open transition, when tuning the laser frequency in resonance with this transition, it has not been possible to observe enhanced-absorption (bright) magneto-optical resonances. In the ETC, however, a large amplitude magneto-optical resonance is observed when the laser frequency is tuned to the center of the transition. But instead of a bright resonance, a dark resonance appears at the $F_g = 3 \rightarrow F_e = 4$ transition, in agreement with the theoretical model. Both the theoretical and experimental resonance profiles are illustrated in Fig.9 for irradiation by linearly polarized light. Here also the scanned magnetic field is oriented in a direction orthogonal to the light polarization and propagation direction. In the case of this resonance, the theory is also in very good quantitative agreement with the experiment related to the dependance of the resonance amplitude on the laser power density. Here, we observe in the magneto-optical resonance width a discrepancy between the theory and the experiment that is even larger than in the

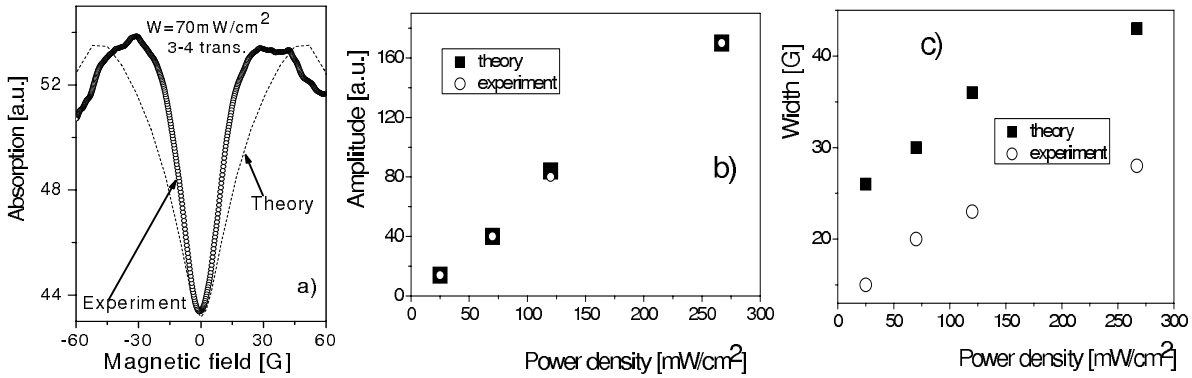

FIG. 9: Comparison between theory and experiment, for $F_g = 3 \rightarrow F_e = 4$ transition and excitation by linearly polarized light: (a) - magneto-optical resonance experimental and theoretical profiles; (b) - magneto-optical resonance amplitude as a function of the light power density; (c) - magneto-optical resonance width as a function of power density.

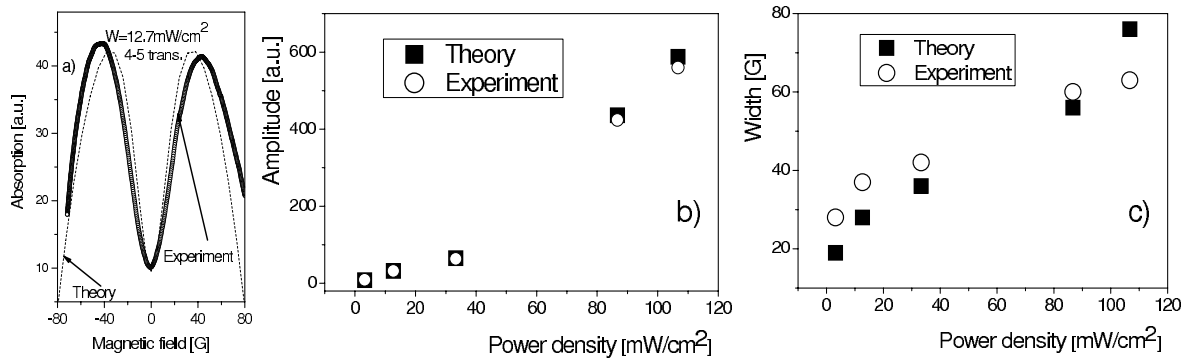

FIG. 10: Comparison between theory and experiment, for $F_g = 4 \rightarrow F_e = 5$ transition and excitation by circularly polarized light: (a) - magneto-optical resonance experimental and theoretical profiles; (b) - magneto-optical resonance amplitude as a function of the light power density; (c) - magneto-optical resonance width as a function of power density.

previous case. The experimentally observed resonance is significantly narrower than the theoretical one. The origin of this discrepancy can be attributed to the fact that the $F_g = 3 \rightarrow F_e = 4$ transition is an open transition. Therefore, a significant population loss occurs from the $F_g = 3$ level to the $F_g = 4$ level as a result of the hf optical pumping through spontaneous transitions from the $F_e = 4$ level. In [24, 25, 26], it has been shown that, in the case of open hf transitions, a significant coherent resonance narrowing takes place, because the resonance destruction is more effective at the wings, while at the center the resonance is more resistant to the loss.

Based on the results presented in Fig.9, we can conclude that, unlike the dark magneto-optical resonance, the bright resonance is very sensitive, not only to the depolarization collisions of alkali atoms with those of the buffer gas in the ordinary cell, but also to the surface - atom interactions, about which it can provide valuable information.

In order to confirm the sensitivity of the $F_g \rightarrow F_e = F_g + 1$ type of transitions to the depolarizing influence of the ETC windows, the behaviour of the closed and high-probability $F_g = 4 \rightarrow F_e = 5$ transition is investigated in detail by irradiating Cs atoms with linearly or circularly polarized light. In the first case the scanned magnetic field is oriented orthogonally to the atomic alignment, while in the second case, orthogonally to the orientation of atoms. In both cases reduced-absorption magneto-optical resonance is observed experimentally for atoms confined in the ETC. Expanding the discussion related to Fig.7, it can be pointed out that in case of dilute atoms confined in the ordinary cell at $B = 0$, irradiation by linearly polarized light also results in atomic accumulation in the ground-state Zeeman sublevels with the highest excitation probabilities. And similar to the case of circular polarization, also in case of linear polarization the excited state depolarization by alkali atom collisions with buffer gas atoms results in a sign reversal of the magneto-optical resonance.

The results obtained from studies with both polarization excitations and with the laser frequency tuned to the central frequency of the $F_g = 4 \rightarrow F_e = 5$ transition, confirm the assumed analogy between the excited state depolarization by atomic collisions (for the ordinary cell) and its depolarization by the influence of the electrical potential of the ETC window. In Fig.10, a comparison between the experimental and theoretical results is presented for the $F_g = 4 \rightarrow F_e = 5$ transition, in

case of Cs atoms irradiated by circularly polarized light with a magnetic field applied in a direction orthogonal to the light propagation. It can be seen that in relation to the magneto-optical resonance width, the agreement between the theory and the experiment is better for the $F_g = 4 \rightarrow F_e = 5$ transition. The reason for this can be the fact that, unlike the $F_g = 3 \rightarrow F_e = 4$ transition, the $F_g = 4 \rightarrow F_e = 5$ transition is a closed one, and so the resonance narrowing due to the population loss is not expected for the last transition.

VII. CONCLUSION

We have presented an experimental and theoretical study of the ground-state magneto-optical resonances prepared in Hanle configuration on the D_2 line of Cs. In a cm-scale ordinary cell containing Cs vapour, the hyperfine transitions starting from a single ground-state level are strongly overlapped, which is a reason for the mixing of the contribution of different hf transitions that are responsible for the dark and bright magneto-optical resonances. It is shown that the utilization of an Extremely Thin Cell with thickness equal to the wavelength of the irradiating light allows one to examine the formation of a magneto-optical resonance on the individual hf transitions due to the experimentally proven fact that only very slow atoms possess enough interaction time with the light to form the magneto-optical resonance. The fast atoms, exhibiting mainly a single act of absorption during their interaction with the light, do not contribute to the magneto-optical resonance formation.

It is shown that in the ETC, dark (reduced absorption) magneto-optical resonances are observed at $F_g \rightarrow F_e = F_g - 1$, F_g transitions, much like in ordinary cells. However in case of the $F_g \rightarrow F_e = F_g + 1$ transitions, Cs atoms confined in ETC exhibit completely different behaviour as compared to those contained in an ordinary cell. For the latter, bright (enhanced absorption) magneto-optical resonances have been observed in dilute Cs vapour in the ordinary cell. As a result of our study we report on the bright resonance sign reversal in Cs atoms confined in the ETC. Both ($F_g = 3 \rightarrow F_e = 4$ and $F_g = 4 \rightarrow F_e = 5$) intrinsically "bright" hf transitions are responsible for dark magneto-optical resonance formation in the ETC.

A theoretical model is proposed based on the optical Bloch equations that involves the elastic interaction processes of atoms in the ETC with its walls. The assumed elastic collisions of Cs atoms with the cell walls do not affect the ground state of alkali, do not reorient the electronic and nuclear spins of the atom, but do affect the excited-state Zeeman coherences and populations, as well as the optical coherences. The involvement of elastic collisions of this type results in depolarization of the Cs excited state that had been polarised by the exciting radiation. This depolarization leads to the accumulation of atomic population in ground-state Zeeman sublevels with the lowest probability of excitation, which is opposite to the situation in the ordinary cell, where atoms accumulate on the Zeeman sublevel possessing the largest probability of excitation. Hence, the influence of the ETC wall on atomic polarization leads to the sign reversal of bright resonance. Using the proposed model, the magneto-optical resonance amplitude and width dependences on laser power are calculated and compared with the experimental ones. The numerical results are in good agreement with the experiment.

The obtained results show that the magneto-optical resonances observed in the ETC could potentially be applied to study atom-surface interactions.

VIII. ACKNOWLEDGEMENTS

The authors are grateful to Prof. D. Sarkisyan for providing the ETC and for the number of extremely useful discussions, as well as we acknowledge partial support from the INTAS programm (grant: 06 - 1000017 - 9001). C. A., S. C., L. P. and D. S. acknowledge support from the Bulgarian Fund for Scientific Research (grant F-1404/04). A. A., M. A. and K. B. acknowledge support from EU FP6 TOK project LAMOL and European Regional Development Fund project Nr. 2.5.1./000035/018. A. A. and K. B gratefully acknowledge support from the European Social Fund. S.C. appreciates very helpful discussions with Prof. D. Bloch, Prof. M. Ducloy and Prof. Yu. Malakyan related to the particular properties of the atoms confined in the ETC and magneto-optical resonances.

[1] I. Hamdi, P. Todorov, A. Yarovitski, G. Dutier, I. Maurin, S. Saltiel, Y. Li, A. Lezama, T. Varzhapetyan, D. Sarkisyan, M.-P. Gorza, M. Fichet, D. Bloch, and M. Ducloy, Laser Physics **15**, 987 (2005).

[2] D. Sarkisyan, D. Bloch, A. Papoyan, and M. Ducloy, Opt. Commun. **200**, 201 (2001).

[3] D. Sarkisyan, T. Becker, A. Papoyan, P. Theumany, and H. Walter, Appl. Phys. **B76**, 625 (2003).

[4] G. Dutier, A. Yarovitski, S. Saltiel, A. Papoyan, D. Sarkisyan, D. Bloch, and M. Ducloy, Europhys. Lett. **63**, 35 (2003).

[5] R. H. Romer and R. H. Dicke, Phys. Rev. **99,** 532 (1955).

[6] D. Sarkisyan, T. Varzhapetyan, A. Sarkisyan, Yu.

Malakyan, A. Papoyan, A. Lezama, D. Bloch, and M. Ducloy, Phys. Rev. **A69**, 065802(2004).

[7] Y.Dancheva, G.Alzetta, S.Cartaleva, M.Taslakov, and Ch.Andreeva, Opt. Commun. **178**, 103(2000).

[8] F. Renzoni, C. Zimmermann, P. Verkerk, and E. Arimondo, J. Opt. B: Quantum Semiclass. Opt. **3**, S7 (2001).

[9] A. Papoyan, M. Auzinsh, and K. Bergmann, Eur. Phys. J. **D21**, 63 (2002).

[10] J. Alnis, K. Blushs, M. Auzinsh, S. Kennedy, N. Shafer-Ray, and E.R.I. Abraham, Journal of Physics B-Atomic Molecular and Optical Physics, **36**, 1161 (2003).

[11] J.Alnis, and M. Auzinsh, Journal of Physics B-Atomic Molecular and Optical Physics, **34**, 3889 (2001).

[12] C.Andreeva, S.Cartaleva, Y.Dancheva, V.Biancalana, A.Burchianti, C.Marinelli, E.Mariotti, L.Moi, and K.Nasyrov, Phys.Rev. **A66**, 012502 (2002).

[13] I. Maurin, P.Todorov, I. Hamdi, A. Yarovitski, G. Dutier, D. Sarkisyan, S. Saltiel, M.-P. Gorza, M. Fichet, D. Bloch, and M. Ducloy, J. of Physics: Conference Series **19**, 20 (2005).

[14] S.Briaudeau, D. Bloch, and M. Ducloy, Phys. Rev. **A59**, 3723 (1999).

[15] D.V. Brazhnikov, A.M. Tumaikin, V.I. Yudin, and A.V.Taichenachev, J. Opt. Soc. Am. **B22**, 57 (2005).

[16] D. V. Brazhnikov, A. V. Taichenachev, A. M. Tumaikin, V. I. Yudin, S. A. Zibrov, Ya. O. Dudin, V. V. Vasil'ev, and V. L. Velichansky, JETF Letters **83**, 64 (2006).

[17] S.Stenholm, *Foundations of laser spectroscopy* (Dover Publications, Inc.,Mineola, New York, 2005).

[18] M.Auzinsh and R.Ferber, *Optical Polarization of Molecules* (Cambridge University Press, Cambridge, 2005).

[19] D.A.Varshalovich, A.N.Moskalev, and V.K.Khersonskii, *Quantum Theory of Angular Momentum* (World Scientific, Singapore, 1988).

[20] R.N. Zare, *Angular Momentum, Understanding Spatial Aspects in Chemistry and Physics* (J.Wiley and Sons, New York, 1988).

[21] L.Allen and J.H.Eberly, *Optical resonance and two level atoms* (Wiley, New York, 1975).

[22] N.G.van Kampen, Phys. Rep. **24**, 171 (1976).

[23] 19. K. Blush and M. Auzinsh, Phys. Rev. **A69**, 063806 (2004).

[24] F. Renzoni and E. Arimondo, Europhys. Lett. **46**, 716 (1999).

[25] F. Renzoni, A. Lindner, and E. Arimondo, Phys. Rev. **A60**, 450 (1999).

[26] F. Renzoni and E. Arimondo, Phys. Rev. **A58**, 4717 (1998).